2-25-1986

Small-Angle X-Ray Scattering Analysis Of Catalysts: Comparison and Evaluation Of Models

H. Brumberger
Syracuse University

F. Delaglio
Syracuse University

Jerry Goodisman
Syracuse University

M. Whitfield
Syracuse University

Recommended Citation

Brumberger, H., Delaglio, F., Goodisman, J., & Whitfield, M. (1986). SMALL-ANGLE X-RAY SCATTERING ANALYSIS OF CATALYSTS: COMPARISON AND EVALUATION OF MODELS. Journal of Applied Crystallography, 19(pt 5), 287-299.

J. Appl. Cryst. (1986). **19**, 287–299

Small-Angle X-ray Scattering Analysis of Catalysts: Comparison and Evaluation of Models

BY H. BRUMBERGER, F. DELAGLIO, J. GOODISMAN AND M. WHITFIELD

Department of Chemistry, Syracuse University, Syracuse, New York 13210, *USA*

(*Received* 13 *November* 1985; *accepted* 25 *February* 1986)

Abstract

Small-angle X-ray scattering (SAXS) can be used to obtain interphase surface areas of a system, such as a supported-metal catalyst, composed of internally homogeneous phases with sharp interphase boundaries. Measurements of SAXS for samples of porous silica, alumina, platinum on silica, and platinum on alumina are reported. A variety of models and forms for the correlation function, the Fourier transform of which gives the X-ray scattering, are considered, and theoretical and measured intensities are compared. A criterion of fit for comparing models with different numbers of parameters is proposed. For the two-phase (unmetallized) systems the 'Debye-random' model must be rejected. Modifications of the Debye (exponential) correlation function are also not particularly good compared to an exponential-plus-Gaussian form, not derivable from a physical model, and forms based on Voronoi cell models. Since intensities can be fit to experimental error with a five-parameter correlation function, it seems incorrect to ascribe significance to the result of fitting a function with six or more parameters. It is shown that values for the single interphase surface area can be obtained independently of a model. However, fitting intensities using a model-based correlation function gives information about the structure of the system. The two-cell-size Voronoi and the correlated Voronoi cell models are useful in this regard. For the systems containing metal, five-parameter correlation functions again suffice to fit intensities. However, for three-phase systems a model or physical assumption is necessary to obtain values for the three surface areas from X-ray scattering intensities. The area of the surface between support and void is quite insensitive to the assumptions employed and the metal–support surface area somewhat less so, but values for the metal–void surface area S_{23} are consistent only to one significant figure from model to model. If the support in the three-phase catalyst is known to be unchanged from support in the absence of metal, a 'support-subtraction' model can be used to obtain reliable values for S_{23}. In the present systems, the assumption does not seem to be borne out.

I. Introduction, basic formulas and experimental details

The small-angle X-ray scattering from a non-crystalline system (Porod, 1951; Debye, Anderson & Brumberger, 1957; Porod, 1982) is proportional to the Fourier transform of the electron density correlation function $\gamma(\mathbf{r})$. Here

$$\gamma(\mathbf{r}) = \int \eta(\mathbf{x})\eta(\mathbf{x}+\mathbf{r})\mathrm{d}\mathbf{x}/V\overline{\eta^2}, \qquad (1)$$

where the integration is over the illuminated volume V, $\eta(\mathbf{x}) = n(\mathbf{x}) - \bar{n}$, $n(\mathbf{x})$ is the electron density at $\mathbf{x}$ and overbars indicate averages over V. For a system composed of internally homogeneous phases with sharp interphase boundaries, $\gamma(\mathbf{r})$ contains information about interphase surface areas, so that small-angle X-ray scattering (SAXS) can be used to measure these areas, instead of gas adsorption, which is known to have certain problems. However, it is not possible to derive surface areas for systems with more than two phases directly from the scattering intensity, without a model for the electron density distribution. From a model one can calculate $\gamma(\mathbf{r})$ and the X-ray scattering as a function of scattering angle, for comparison with experimental scattering; then one can calculate interphase surface areas for the model. We will be concerned with ascertaining how well different models fit, and how much information one can really obtain by fitting to a model. One will then be able to delineate the physically realistic and practical framework within which these models, and indeed scattering models in general, are useful.

The systems we consider are spatially isotropic, so that $\gamma(\mathbf{r})$ is a function only of the magnitude r, and the scattering intensity is a function only of $h = 4\pi(\sin\theta)/\lambda$; θ = half the scattering angle. For a point-collimated source, the intensity is (Ruland, 1971; Brumberger, 1983)

$$I(h) = \overline{\eta^2} V I_e(h) \int 4\pi r^2 (\sin hr)(hr)^{-1}\gamma(r)\mathrm{d}r, \qquad (2)$$

where $\overline{\eta^2}$ is the mean-square electron-density fluctuation and $I_e(h)$ is

$$I_e(h) = I_0(e^2/mc^2)^2(1+\cos^2 2\theta)/2l^2,$$

0021-8898/86/050287-13$01.50

with I_0 the incident intensity and l the sample-to-detector distance; for the range of θ investigated here, $I_e(h)$ may be taken as a constant. For a primary beam collimated with an infinitely long uniform slit, the scattered intensity is

$$\tilde{I}(h) = \int_{-\infty}^{\infty} I[(h^2 + s^2)^{1/2}]\mathrm{d}s$$

$$= \overline{\eta^2} V I_e(h) 4\pi^2 \int_0^{\infty} J_0(hr) r\gamma(r)\mathrm{d}r. \qquad (3)$$

We refer to the calculation of $\tilde{I}$ from I as slit smearing. Since we do not measure absolute intensities, $V\overline{\eta^2} I_e(h)$ is not known, and we take it as an unknown constant C.

In fact, our primary beam is not of uniform intensity, but has a trapezoidal intensity profile. Thus, what we measure experimentally is not $\tilde{I}(h)$ but

$$\bar{I}(h) = 2\int_0^{\infty} w(s) I[(h^2 + s^2)^{1/2}]\mathrm{d}s, \qquad (4a)$$

where

$$w(s) = 1,\ s < s_1;\ w(s) = (s - s_2)/(s_1 - s_2),\ s_1 \le s \le s_2;$$

$$w(s) = 0,\ s > s_2. \qquad (4b)$$

The values of s_1 and s_2 are known from measurements. The derivation of quantities related to $\tilde{I}(h)$ from measured $\bar{I}(h)$ will be discussed below.

It is convenient, for our systems, to introduce (Goodisman & Brumberger, 1971) the stick probability functions $P_{ij}(r)$: $P_{ij}(r)$ is the probability that a stick of length r, placed at random in the system, will have end A in phase i and end B in phase j. For an N-phase system, there are N^2 P_{ij}'s of which $\frac{1}{2}N(N-1)$ are independent, since $P_{ij} = P_{ji}$ and $\sum_j P_{ij} = \varphi_i$ (Goodisman & Brumberger, 1979). In terms of the independent stick probability functions,

$$\gamma(r) = 1 - \frac{\sum_{ij} P_{ij}(r)(n_i - n_j)^2}{\sum_{ij} \varphi_i \varphi_j (n_i - n_j)^2}. \qquad (5)$$

Note that $P_{ij}(0) = 0$ for $i \neq j$ and $P_{ij}(\infty) = \varphi_i \varphi_j$ so $\gamma(0) = 1$ and $\gamma(\infty) = 0$. The interphase surface areas obey (Goodisman & Brumberger, 1971)

$$S_{ij}/4V = (\mathrm{d}P_{ij}/\mathrm{d}r)_{r=0} \qquad (6)$$

while the second derivative of P_{ij} at $r = 0$ is related (Ciccariello, Cocco, Benedetti & Enzo, 1981) to the angularity of the corresponding surface. It is also useful to write (Ciccariello & Benedetti, 1985)

$$\gamma(r) = \sum_{i<j} \gamma_{ij} Q_{ij} \qquad (7)$$

with

$$\gamma_{ij} = (\varphi_i \varphi_j - P_{ij})/\varphi_i \varphi_j \qquad (8a)$$

and

$$Q_{ij} = \varphi_i \varphi_j (n_i - n_j)^2 / \sum_{k<l} \varphi_k \varphi_l (n_k - n_l)^2 \qquad (8b)$$

so that $\sum_{i<j} Q_{ij} = 1$. The Q_{ij}, like φ_i and n_i, are parameters whose values are known independently of the X-ray experiments.

The four systems considered are: (1) silica gel, a two-phase system, the second phase being void; (2) platinum dispersed on the silica gel of system (1); (3) γ-alumina; (4) platinum dispersed on the alumina of (3) as support. The electron densities and volume fractions for the four samples are given in Table 1 (Nandi, Molinaro, Tang, Cohen, Butt & Burwell, 1982).

The scattering of these samples was measured with a modified Kratky camera in the 'infinite slit' geometry and a one-dimensional position-sensitive detector. Ni-filtered Cu $K\alpha$ radiation was employed in conjunction with pulse-height discrimination. Background scattering, corrected for sample transmission, was subtracted from sample scattering in the angular range where it made significant contributions.

Accumulated counts varied from over 2×10^5 at the smallest scattering angles to about 400 at the largest experimentally accessible angles (most probable error ranging from ~0·2 to ~5%). The angular variable h ranged from ~0·010 to ~0·200. The most probable error in this region varied from $\lesssim$1·8 to ~5%. All scattering curves displayed a well developed high-angle region $h \gtrsim$ ~0·100, where the slit-smeared intensities varied as h^{-3} (Porod's law region) (Figs. 1 and 2). A plot of $h\tilde{I}(h)$ *vs* h showed a well defined maximum which allowed us to extrapolate to $h = 0$

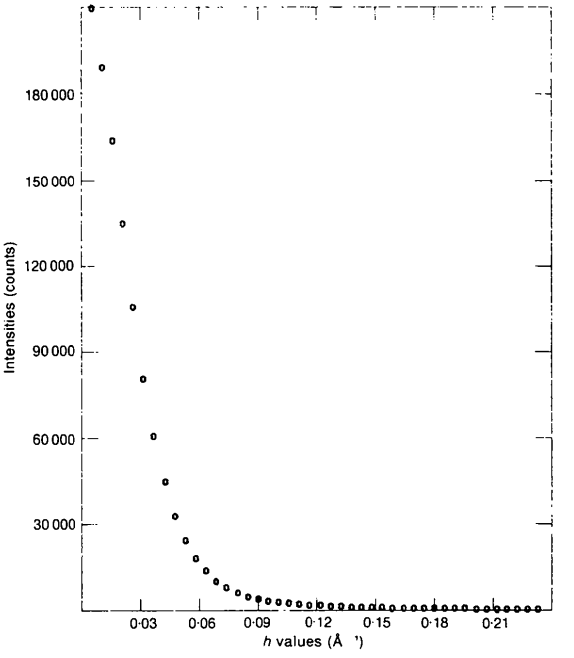

Fig. 1. Some of the experimental intensities for SiO_2 as a function of h. Data for other substances are similar.

Table 1. *Sample characteristics*

Sample	Mass density (g cm^{-3})	Volume fractions*			Electron densities*†		
		φ_1	φ_2	φ_3	n_1	n_2	n_3
SiO_2	0·3843	0·1755	0·8245	0·0	1·093	0·0	–
SiO_2 + 2% Pt	0·3882	0·17544	0·8242	0·00036	1·093	0·0	8·576
Al_2O_3	0·6486	0·1753	0·8247	0·0	1·814	0·0	–
Al_2O_3 + 4% Pt	0·6638	0·17509	0·82372	0·00118	1·814	0·0	8·576

These samples were received from the laboratory of Professor J. B. Cohen, Northwestern University, where density and other characterization measurements were also performed. (See also Nandi *et al.*, 1982.) We are most grateful to Professor Cohen and Dr R. K. Nandi for sending us these samples and measurements.

*Phase 1 = support, phase 2 = void, phase 3 = metal.

†In mol of electrons cm^{-3}.

with confidence and obtain a reliable value for $\tilde{Q} = \int_0^\infty h\tilde{I}(h)dh$ (Fig. 3).

For a two-phase system, the interphase surface-to-volume ratio can be determined from the X-ray scattering data without the necessity of a model, but we shall consider a series of models to ascertain how well they fit the scattering data and how many parameters are required to fit the data. For a system of more than two phases, one cannot obtain individual surface areas *without* a model. Again, a series of models will be investigated and compared. Theories which use the scattering of the support (SiO_2) in conjunction with that of the catalyst (SiO_2 + Pt) will also be considered.

From a model for the scattering system, one can calculate $\gamma(r)$ and, from $\gamma(r)$, the scattering intensity $\tilde{I}(h)$ according to (3). Then, if the fit between experimental ($\tilde{I}$) and calculated ($\tilde{I}_t$) intensities is sufficiently good, we derive surface areas from the P_{ij} of the model. Generally, γ will include several parameters, whose values will be chosen to optimize the fit between experimental and calculated intensities. Our criterion of fit, which we minimize with respect to the parameters in $\gamma(r)$, is

$$Q = \sum_i [\tilde{I}(h_i) - \tilde{I}_t(h_i)]^2/\tilde{I}(h_i), \tag{9}$$

where the h_i are the h values for which intensities are given. Minimizing the sum of squared deviations would give a good fit only for high intensities. In the absence of absolute intensities, $\tilde{I}_t$ will always include a multiplying parameter corresponding to C, so that

$$I_t = C \int \exp(i\mathbf{k}.\mathbf{r})\gamma_t(r)d\mathbf{r} \tag{10}$$

with $\gamma_t(0) = 1$. By examining values of Q for various choices of γ_t, we can assess the applicability of models to the system being considered.

Naturally, a decrease in Q will result from a model with additional parameters which can be varied to fit $\tilde{I}_t(h)$ as well as possible to $\tilde{I}(h)$. A lower value of Q

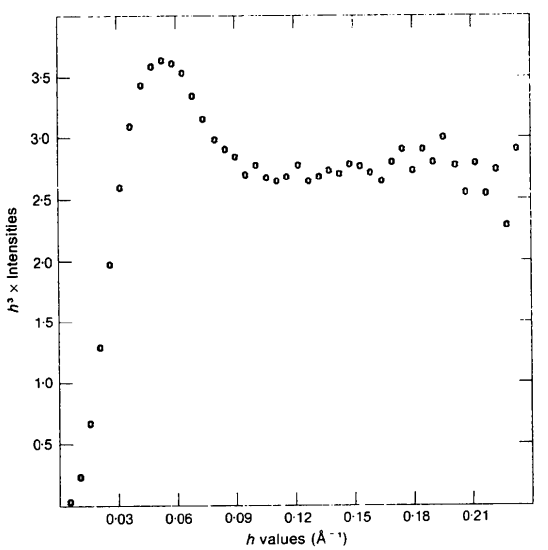

Fig. 2. Intensities for SiO_2 multiplied by h^3, showing Porod's law for large h.

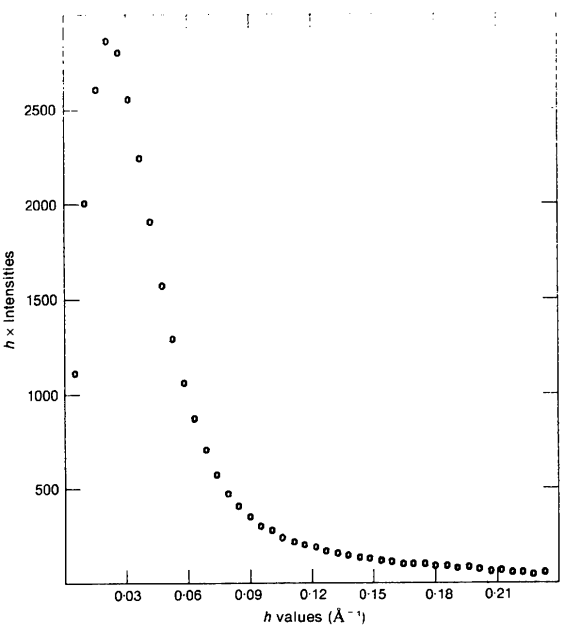

Fig. 3. Intensities for SiO_2 multiplied by h, for calculation of $\int h\tilde{I}(h)dh$.

indicates a better model only when comparison is between two models with the same number of parameters. To compare models with different numbers of parameters, we introduce a figure of merit suggested by that used to discuss linear least-squares fits (Daniel & Wood, 1971). If N_I data points $\tilde{I}_j$ are to be fitted to a function

$$\tilde{I}_t = b_0 + \sum_{i=1}^{K} b_i x_i$$

of the K independent variables x_i by minimizing $\sum(\tilde{I} - \tilde{I}_t)_i^2$ with respect to $K+1$ independent parameters b_i, one defines the 'multiple correlation coefficient squared' as

$$R^2 = \left[\sum (\tilde{I} - I_t)_i^2\right] \Big/ \left[\sum (\tilde{I}_i - \bar{I})^2\right],$$

where $\bar{I}$ is the mean value of $\tilde{I}_i$. Then the significance of the fit is calculated by multiplying $R^2/(1-R^2)$ by $(N_I - K - 1)/K$, so that the significance increases as R decreases but, if the same R is obtained from two fits, the one with the smaller K is considered more significant. To modify this for our purpose, we note that instead of minimizing the sum of $(I_t - \tilde{I})_i^2$ we minimize Q. Thus, R^2, which is to be dimensionless, is replaced by

$$S^2 = 1 - Q/\sum_i |\tilde{I}_i - \bar{I}|,$$

where $N_I \bar{I} = \sum \tilde{I}_i$. Then we take as our figure of merit for significance

$$F = [S^2/(1-S^2)][(N_I - P)/(P-1)], \qquad (11)$$

where P is the number of parameters. As $S \to 0$ (perfect fit), $F \to \infty$; F decreases as P increases, becoming 0 if the number of parameters becomes equal to the number of intensities fitted.

As noted above, our experimental intensities actually represent $\bar{I}(h)$ of (4) rather than intensities for an infinitely long slit-collimated beam. In order to choose parameters in a theoretical correlation function γ_t to minimize Q, (9) should be replaced by

$$\sum_i [\bar{I}(h_i) - \bar{I}_t(h_i)]^2/\bar{I}(h_i)$$

and

$$\bar{I}_t(h) = \tilde{I}_t(h) + 2\int_0^\infty [w(s) - 1] I[(h^2 + s^2)^{1/2}] \mathrm{d}s$$

with $\tilde{I}_t(h)$ calculated from γ_t by (3) and the correction term easily evaluated by noting that $I(h) \sim -4\pi C h^{-4}\gamma_t'(0)$ [see (13)] for all h for which $w(s) \neq 1$. Then

$$-8\pi C\gamma_t'(0)\int_{s_1}^\infty [w(s)-1](h^2+s^2)^{-2}\mathrm{d}s$$
$$= -[8\pi C\gamma_t'(0)/(s_1 - s_2)h^3][s_1 \tan^{-1}(s_1/h) - s_2 \tan^{-1}(s_2/h) - \pi(s_1 - s_2)/2].$$

Thus, in evaluating Q we use experimental intensities for $\tilde{I}(h)$ and add the above correction to $\tilde{I}_t(h)$, (3).

II. Two-phase system

For a two-phase system we have, according to (4) and (5),

$$S/4V = -\varphi_1\varphi_2(\mathrm{d}\gamma/\mathrm{d}r)_{r=0}. \qquad (12)$$

The initial slope of γ may be determined directly from the X-ray intensities. Thus, integrating (2) by parts several times, one finds (Porod, 1982; Brumberger, 1983)

$$I(h) = C[-4\pi h^{-4}\gamma'(0) \ldots], \qquad (13)$$

where $C = VI_e(h)\overline{\eta^2}$. Then, on slit smearing, we find that $\tilde{I}(h)$ approaches $-2\pi^2 C\gamma'(0)/h^3$ as h approaches infinity, so

$$\tilde{k} \equiv \lim_{h\to\infty} h^3\tilde{I}(h) = C[-2\pi^2\gamma'(0)]. \qquad (14)$$

The value of C may be obtained from

$$\tilde{Q} \equiv \int_0^\infty h\tilde{I}(h)\mathrm{d}h = 2\int_0^\infty \mathrm{d}u u^2 I(u)$$
$$= 2(4\pi)^{-1}\int \mathrm{d}\mathbf{u} I(\mathbf{u}).$$

Since

$$(4\pi)^{-1}C\int \mathrm{d}\mathbf{u}\int \mathrm{d}\mathbf{r}\exp(i\mathbf{u}.\mathbf{r})\gamma(\mathbf{r})$$
$$= (4\pi)^{-1}C\int \mathrm{d}\mathbf{r}\gamma(\mathbf{r})(2\pi)^3\delta(\mathbf{r})$$

and $\gamma(0) = 1$, we have $\tilde{Q} = (2\pi^2)C$ so that

$$\tilde{k}/\tilde{Q} = -\gamma'(0) \qquad (15)$$

independent of any model.

As mentioned earlier, our data do not correspond to an infinite-slit collimated beam, but rather represent $\bar{I}(h)$ of (4). To extract $\tilde{k}$, we note that, according to (13) and (14), if $\tilde{I}(h) \to \tilde{k}/h^3$ for $h \to \infty$, $I(h) \to 2\tilde{k}/\pi h^4$, so that

$$\bar{I}(h) \to 2\int_0^\infty w(s)2\tilde{k}\pi^{-1}(h^2+s^2)^{-2}\mathrm{d}s$$
$$= [2\tilde{k}/\pi h^3(s_1 - s_2)][s_1\tan^{-1}(s_1/h) - s_2\tan^{-1}(s_2/h)]$$
$$\equiv \tilde{k}\bar{I}_a(h),$$

which approaches $\tilde{k}/h^3$ for $h \ll s_1 < s_2$. By dividing our experimental scattering intensities by $\bar{I}_a(h)$ (and verifying that the ratio becomes constant for larger h values) we find $\tilde{k}$. To determine $\tilde{Q}$, we first determine

$$Q^1 = \int_0^u \mathrm{d}h h\bar{I}(h) \quad (u > s_2)$$

by numerical integration of our data. Then we take

Table 2. *Functions for two-phase systems*

Function	Equation	Fit to SiO_2 data Q	S^2	$F/1000$	Fit to Al_2O_3 data Q	S^2	$F/1000$
Debye-random	(16), (17)	$(2{\cdot}49 \times 10^4)$	0·9826	2	$(3{\cdot}3 \times 10^4)$	0·9817	2
Two exponentials	(18)	2504	0·9984	9	3247	0·9984	9
Gaussian + exponential	(19), (20)	303	0·9998	74	502	0·9998	56
Exponential-sine	(21)	3864	0·9976	9	5572	0·9972	8
Exponential-cosine	(22)	7247	0·9955	5	$(1{\cdot}04 \times 10^4)$	0·9948	4
Voronoi cell	(23), (24)	5666	0·9964	12	8791	0·9958	10
Two Voronois	(26)	157	0·9999	142	311	0·9998	93
Three Voronois	(23), (26)	84	0·9999	130	276	0·9999	58
Correlated Voronoi	(32), (38)	2956	0·9981	12	3169	0·9984	14

advantage of the fact that the asymptotic $(2\tilde{k}/\pi h^4)$ behavior of $I(h)$ is already attained for $h \geq s_1$. This means that

$$\begin{aligned}\tilde{Q} - Q^1 &= \int_u^\infty \mathrm{d}hh\tilde{I}(h) + \int_0^u \mathrm{d}hh[\tilde{I}(h) - \bar{I}(h)] \\ &= \int_u^\infty \mathrm{d}hh(\tilde{k}/h^3) + 2\int_0^u \mathrm{d}hh \\ &\quad \times \int_{s_1}^\infty \mathrm{d}s[1 - w(s)]2\tilde{k}\pi^{-1}(h^2 + s^2)^{-2} \\ &= \tilde{k}u^{-1} + 2\tilde{k}\pi^{-1}\int_{s_1}^\infty \mathrm{d}s[1 - w(s)] \\ &\quad \times [s^{-2} - (u^2 + s^2)^{-1}].\end{aligned}$$

Explicitly,

$$\begin{aligned}\tilde{Q} = Q^1 + 2\tilde{k}\pi^{-1}(s_1 - s_2)^{-1}\{&(s_1/u)\tan^{-1}(s_1/u) \\ &- (s_2/u)\tan^{-1}(s_2/u) - \ln(s_2/s_1) \\ &+ \tfrac{1}{2}\ln[(u^2 + s_2^2)/(u^2 + s_1^2)]\}.\end{aligned}$$

Our procedure is to determine $\tilde{k}$ using $\bar{I}_a(h)$ and then $\tilde{Q}$ by the above formula.

For amorphous SiO_2 we find $\tilde{k} = 3{\cdot}38(18)$ Å^{-3} [the error is the mean-square deviation in values of $\tilde{I}(h)/\bar{I}_a(h)$ in the appropriate h range] and 152·6 Å^{-2} for the integral of $h\bar{I}(h)$ from $h = 0$ to $h = 0{\cdot}2387$. The correction $\tilde{Q} - Q^1$ is 17·3, so that $\tilde{Q} = 170{\cdot}0$, $\gamma'(0) = 0{\cdot}01987$ Å^{-1} and $S/V = 0{\cdot}001149(61)$ Å^{-1} using (12) and (15). The specific surface is obtained by dividing by the bulk density (0·3843 g cm^{-3}): $S^* = 299(16)$ m^2 g^{-1}. The BET absorption measurements of Nandi *et al.* (1982) gave 285 m^2 g^{-1}, while the SAXS result was 327 m^2 g^{-1}.

Applying the same analysis to the alumina support, we find that $k = 4{\cdot}013(260)$ Å^{-3}, $\tilde{Q} = 213{\cdot}92$, so $\gamma'(0) = 0{\cdot}01876(150)$ Å^{-1} and $S_{12}/V = 0{\cdot}01082(75)$ Å^{-1}. Using the mass density given in Table 1 we have a specific surface of 166(13) m^2 g^{-1}. Nandi (1984) reported 160 m^2 g^{-1} from BET measurements and 222 m^2 g^{-1} from SAXS measurements. We now turn to expressions for the correlation function.

(a) Fitting functions

The simplest model, at least computationally, is the 'Debye-random' model (Goodisman & Brumberger, 1971, 1979; Ciccariello, 1983), which leads to a correlation function

$$\gamma(r) = \exp(-r/a). \tag{16}$$

The form of γ is obtained by considering $\mathrm{d}P_{ij}/\mathrm{d}r$: this quantity differs from zero according to the probability that an end of a stick of length r is near an interphase surface, so that extending r to $r + \mathrm{d}r$ leads to a crossing from one phase to another. The assumption that the probability of being near a surface is just the surface-to-volume ratio yields linear differential equations for the P_{ij} whose solution (Goodisman & Brumberger, 1971) corresponds to (16). With the constant C, this model involves two parameters. The calculated intensity is

$$\tilde{I}_t = C(4\pi^2 a^2)(1 + h^2 a^2)^{-3/2}. \tag{17}$$

On optimization, we find for SiO_2 that $Q = 2{\cdot}49 \times 10^4$. Since the intensities $\tilde{I}(h)$ vary from $2{\cdot}095 \times 10^5$ to 183, this value of Q does not represent a good fit. The value of the parameter a found by fitting intensities is 37·03 Å, so that $\gamma'(0) = -0{\cdot}0270$ Å^{-1}, which is 36% higher than the value determined from the experimental data. This confirms that this model is a poor one for this system. The values of S^2 and F (11) are given in Table 2.

It is computationally easy to generalize (16) to a sum of exponentials

$$\gamma(r) = f\exp(-r/a) + (1 - f)\exp(-r/b) \tag{18}$$

for which $\tilde{I}(h)$ is a sum of functions like (17). Minimizing Q with respect to the four parameters involved, we find Q much lower than for the single exponential, but, since the number of variable parameters has been doubled, F (see Table 2) is not improved as much. Considering what we obtain for F with other four-parameter functions, below, (18) is a poor representation of the correlation function for this system. Our best fit was obtained with $a = 22{\cdot}9$, $b = 24{\cdot}17$ Å, $f = -13{\cdot}22$, $C = 4{\cdot}13$ and yielded $\gamma'(0) = 0{\cdot}5770 - 0{\cdot}5883 = -0{\cdot}0114$ Å^{-1}, which is poor. The value of $\gamma'(0)$ is very

sensitive to the value of f, since it is the difference between two large numbers.

Another four-parameter function involves a Gaussian (Peterlin, 1965). Like a sum of exponentials, it is computationally easy but without theoretical justification in terms of a model:

$$\gamma(r) = f\exp(-r/a) + (1-f)\exp(-r^2/b^2). \quad (19)$$

The Fourier transform and slit-smearing of (19) leads to

$$\tilde{I}_t(h) = Cf[4\pi^2a^2/(1+a^2h^2)^{3/2}] + C(1-f)2\pi^2b^2\exp(-b^2h^2/4). \quad (20)$$

On optimizing the four parameters to minimize Q we find $a = 34{\cdot}30$, $b = 55{\cdot}00$ Å, $C = 4{\cdot}197$, $f = 0{\cdot}6321$. Remarkably, Q is now 502, much lower than for two exponentials. We consider this function as affording a very good fit to $\gamma(r)$. The value of $\gamma'(0)$ (note that the slope of a Gaussian vanishes at the origin) is $-0{\cdot}01821$ Å^{-1}, quite close to that found from $\tilde{k}/\tilde{Q}$ [$-0{\cdot}01987(110)$ Å^{-1}].

Ciccariello (1984) proposed to modify the exponential form in two ways: the exponential-sine function is

$$\gamma(r) = \exp(-r/a)\sin(r/b)/(r/b) \quad (21)$$

and the exponential-cosine function is

$$\gamma(r) = \exp(-r/a)\cos(r/b). \quad (22)$$

These functions, suggested by the correlation function for a hard-sphere liquid, can be Fourier transformed and slit-smeared to give $\tilde{I}_t(h)$ analytically. Including C, $\tilde{I}_t(h)$ contains three parameters. For our SiO_2 data, we find that (21) fits best with $a = 49{\cdot}86$ and $b = 47{\cdot}73$ Å, giving $Q = 3864$. Comparing this to what we obtained from the four-parameter exponential + Gaussian (19), we consider that the fit is not particularly good. The initial slope is easily found to be $-1/a = 0{\cdot}02006$ Å^{-1}, which is 10% higher than $\tilde{k}/\tilde{Q}$. Similarly, (22) gives $Q = 7247$ with $a = 45{\cdot}54$, $b = 100{\cdot}5$ Å; $\gamma'(0) = -0{\cdot}02196$ Å^{-1}, 11% too high compared to $\tilde{k}/\tilde{Q}$. We conclude that neither function is particularly useful for this system. The F values, given in Table 2, bear this out.

Table 2 also shows results for Al_2O_3, using the functions discussed; the conclusions are the same. The exponential correlation functions, and hence the 'Debye-random' model, must be rejected, as they give a poor fit and a poor value of $\gamma'(0)$. An exponential plus a Gaussian is considerably better and gives a value of $\gamma'(0)$ within 10% of the value obtained from $\tilde{k}/\tilde{Q}$, but has no physical significance. The sine-exponential and cosine-exponential functions are not particularly good.

(b) *Voronoi functions*

We will consider in the next subsection correlation functions based on cell models, which assume (Goodisman & Coppa, 1981; Coppa & Goodisman, 1981) that the sample may be thought of as a division of space into cells, each of which is filled with solid SiO_2 or left void. The cells used (Brumberger & Goodisman, 1983) are Voronoi cells, which are generated (Kaler & Prager, 1982) from a random distribution of points in three-dimensional space (Poisson points) by assigning to each point a cell containing all the space closer to that Poisson point than to any other. Each Voronoi cell is bounded by planes bisecting the lines connecting neighboring Poisson points. Their distribution is characterized by a single parameter, c, the density of Poisson points, so that the average volume of a cell is c^{-1}. Their properties have been studied (Meijering, 1953; Kaler & Prager, 1982; Brumberger & Goodisman, 1983) by several authors. An important function is the noncrossing function $p_0(r)$, which is the probability that a stick of length r lies wholly within one cell, crossing no cell boundary. For small r (Brumberger & Goodisman, 1983)

$$p_0(r) = 1 - \tfrac{8}{9}(\tfrac{3}{2})^{2/3}\Gamma(\tfrac{2}{3})\kappa^{1/3} + \tfrac{8}{45}(\tfrac{3}{2})^{1/3}\Gamma(\tfrac{1}{3})\kappa^{2/3} + \ldots \quad (23)$$

with $\kappa = \pi cr^3/4$. Since it is convenient to calculate and tabulate p_0 as a function of $\kappa^{1/3}$, we take $(\pi c/4)^{-1/3}$ as a characteristic length l. Then the slit-smeared Fourier transform of $p_0(r)$ is

$$4\pi^2\int_0^\infty rJ_0(hr)f(r/l)\mathrm{d}r = 4\pi^2l^2\int_0^\infty \chi J_0(hl\chi)f(\chi)\mathrm{d}\chi \equiv 4\pi l^2F(hl)$$

and $F(hl)$ can be tabulated.

We now consider taking $p_0(r)$ as our correlation function, so that

$$\tilde{I}_t = 4\pi Cl^2F(hl) \quad (24)$$

and one chooses the two parameters C and l to minimize Q. The best fit for SiO_2, with $l = 94{\cdot}38$ Å and $C = 4{\cdot}147$ gives $Q = 5666$, which is an order of magnitude better than the other two-parameter function (exponential). To obtain the surface area, we have from (23)

$$\gamma'(0) = p_0'(0) = -(\tfrac{8}{9})(\tfrac{3}{2})^{2/3}\Gamma(\tfrac{2}{3})/l, \quad (25)$$

which gives $-\gamma'(0) = 1{\cdot}57724/94{\cdot}62 = 0{\cdot}01672$ Å^{-1}.

Next we consider fits to sums of Voronoi noncrossing functions with different characteristic lengths. If two such functions are used,

$$\gamma(r) = fp_0(r; l_1) + (1-f)p_0(r; l_2). \quad (26)$$

We find we can reduce Q to 157 with this four-parameter function. Even taking into account the number of parameters (see Table 2, F), it is far superior to any function so far introduced. The initial slope is

$$-\gamma'(0) = 1{\cdot}57224[f/l_1 + (1-f)/l_2] = 0{\cdot}01793 \text{ Å}^{-1} \quad (27)$$

since $f = 0{\cdot}6520$, $l_1 = 75{\cdot}72$, and $l_2 = 126{\cdot}3$ Å. If one then goes to three Voronoi functions, Q can be reduced to 84. We find, on minimization of Q, characteristic lengths of 28·71, 75·94, and 126·6 Å, with corresponding coefficients −0·0145, 0·6433, 0·3422. If one uses these results in a formula like (27), the value of $\gamma'(0)$ is $-0{\cdot}02095$ Å^{-1}. This differs slightly from $\gamma'(0)$ *via* $\tilde{k}/\tilde{Q}$ because, for $l = 28{\cdot}71$ Å, the largest value of h used (0·2387 Å^{-1}) does not make hl large enough for I_t to make on its asymptotic form. The value of F (Table 2) shows the three-Voronoi fit is not better than the two-Voronoi fit if the increased number of parameters is considered.

In fact, we believe this function fits the experimental data as well as they can or should be fitted, because the deviations between theoretical and experimental intensities can be ascribed wholly to experimental uncertainty. Assuming that the error in the number of counts for each value of h, *i.e.* in $\tilde{I}(h)$, is the probable statistical error or the square root of the number of counts (actually the error is larger since there are other sources of error), we calculate, for each value of h,

$$|\tilde{I}(h) - \tilde{I}_t(h)|/\tilde{I}(h)^{1/2} \equiv E(h).$$

The quantity $E(h)$ is less than unity for half the h values and between one and two for about half the remainder, so that the deviations can be accounted for by the statistical error in the measurements. Thus a maximum of six parameters can be used in the theoretical function. [In fact, calculation of $E(h)$ for the four-parameter function (26) shows that the deviations between $\tilde{I}$ and I_t are already almost statistical.] This implies that it would be meaningless to try to extract more information by fitting a function with more parameters to the experimental data, or to interpret the values of the parameters physically.

The scattering of Al_2O_3 can be fit to the functions considered above. The results are summarized in Table 2. The single Voronoi p_0 gives almost as good a fit as the sine-exponential, although the latter involves one more parameter. A sum of two Voronoi noncrossing functions is better than exponential plus Gaussian, which likewise involves four variable parameters in the intensity. With three Voronoi noncrossing functions, and six parameters in the intensity, one can fit ($Q = 276$) the scattering intensities to experimental error, in the sense discussed above, and calculate $\gamma'(0)$ equal to $-0{\cdot}01800$ Å^{-1}, close to what is obtained from $\tilde{k}/\tilde{Q}$.

(c) *Cell models*

The functions considered have been judged by their ability to fit the experimental $\tilde{I}(h)$. They are simply representations of $\gamma(r)$, unless they derive from a picture of the way the electron density is distributed; the surface area can be obtained directly from the $\tilde{I}(h)$. We now consider cell models for these systems. In the simplest of the cell models, we start with a set of Voronoi cells with characteristic length l and assume that each cell is filled with solid or void phase, randomly and independently, such that the known volume fractions φ_1 and φ_2 obtain. Thus φ_i represents the probability that a Voronoi cell contains phase i. It can be shown (Goodisman & Coppa, 1981) that in this case the correlation function is identical to the noncrossing function. Thus the corresponding scattering intensity is given by (24).

For SiO_2, the best fit is obtained when space is divided into Voronoi cells of average volume $c^{-1} = (4l/\pi)^3 = 0{\cdot}1735 \times 10^6$ Å^3, 0·1755 of which, on a random basis, are filled with SiO_2, and the rest are empty. We have proposed (Brumberger & Goodisman, 1983) improvements on this picture, such as a model involving cells of two average sizes: space is divided into cells of average volume c_1^{-1}, some of which are filled with SiO_2 on a random basis. The remainder are divided into cells of average volume c_2^{-1} ($c_2 > c_1$), and a fraction of these are also filled with SiO_2.

If the fact that the small cells may not fit neatly into the large ones is ignored, the correlation function corresponding to this model is obtained (Coppa & Goodisman, 1981) by considering all the situations which contribute to each P_{ij}. The result, on substituting into (4), is

$$\gamma(r) = (1 - g\varphi_1)^{-1}[\varphi_2 g p_0^{(b)} + (1 - g)p_0^{(s)}]. \quad (28)$$

Here, $p_0^{(b)}$ and $p_0^{(s)}$ are Voronoi-cell noncrossing functions for cell parameters l_b and l_s with $l_b > l_s$, and g is the fraction of phase 1 that is present in large cells. The scattering intensity $I_t(h)$ for the correlation function (28) is the same as that for (26). Thus this model, which involves four variable parameters, gives an excellent fit ($Q = 157$ for SiO_2). The parameter f of (26) now corresponds to $\varphi_2 g/(1 - g\varphi_1)$, so

$$0{\cdot}6520(1 - 0{\cdot}8245g) = 0{\cdot}1755g$$

and $g = 0{\cdot}9144$. For Al_2O_3 results are similar. The normalized correlation function is found to be

$$\gamma(r) = 0{\cdot}6889p_0^{(s)}(r) + 0{\cdot}3111p_0^{(b)}(r),$$

where the large and small cell lengths are respectively 133·93 and 75·41 Å [giving $\gamma'(0) = -0{\cdot}01814$ Å^{-1}, 11% too high]; 30% of the alumina is in large cells.

Now for SiO_2 according to this model, $l_b/l_s = 1{\cdot}668$, so that there are about 4·6 small cells in each big cell, and a similar ratio is found for Al_2O_3. This number not being very large, one could question the assumption that edge effects in fitting small cells into large ones may be ignored. A new cell model (Delaglio, Goodisman & Brumberger, 1986) for this system is also an improvement on the simple random cell model, but free from the edge-effect problem. It involves a nonrandom filling of Voronoi cells, so that the likelihood that the neighbors of a silica-containing

cell also contain silica is somewhat different from the average probability (volume fraction of silica).

Let ψ_{ij} be the conditional probability that, given a cell containing phase j, a nearest-neighbor cell (*i.e.* one sharing a face with the first cell) contains phase i. In the random-filling models presented previously, $\psi_{ij} = \varphi_i$. Because of their definition, the conditional probabilities ψ_{ij} obey

$$\psi_{ji}\varphi_i = \psi_{ij}\varphi_j, \tag{29}$$

either expression representing the probability that, given two neighboring cells, one contains phase i and the other phase j. The ψ_{ij} must obey the normalization condition

$$\sum_j \psi_{ij}\varphi_j = \varphi_i = \sum_j \psi_{ji}\varphi_i. \tag{30}$$

Since for an N-phase system there are $\frac{1}{2}N(N-1)$ conditions (29) and N conditions (30), there are $\frac{1}{2}N(N-1)$ independent ψ_{ij}, the same as the number of independent $P_{ij}(r)$.

The correlation function now involves $p_1(r)$, the nearest-neighbor crossing function: $p_1(r)$ is the probability that a stick of length r, randomly thrown into the system, has its two ends in nearest-neighbor cells. From the assumptions of this model,

$$P_{ij}(r) = p_0(r)\varphi_i\delta_{ij} + p_1(r)\psi_{ji}\varphi_i + [1 - p_0(r) - p_1(r)]\varphi_i\varphi_j. \tag{31}$$

If we insert this into (4), we find for the correlation function, after some algebraic manipulation,

$$\gamma(r) = p_0(r) + p_1(r) \times \left[1 - \sum_{ij} \psi_{ji}\varphi_i(n_i - n_j)^2 / \sum_{ij} \varphi_i\varphi_j(n_i - n_j)^2\right]. \tag{32}$$

If $\psi_{ji} = \varphi_j$, $\gamma(r)$ reduces to the random-filling results, $\gamma(r) = p_0(r)$.

The function $p_1(r)$ must obey the following (Delaglio *et al.*, 1986): (*a*) $p_1(r)$ must always lie between 0 and 1, being a probability; (*b*) $p_1(0) = 0$ since a stick of length 0 must lie wholly within one cell; (*c*) $p_1(\infty) \to 0$ since for large distance the probability of crossing only one cell boundary becomes zero; (*d*) $(dp_1/dr)_0 = -(dp_0/dr)_0$ since, as their length increases from zero, the sticks can cross only one cell boundary; (*e*) the integral of $p_1(r)$ over all space must yield the average value of NV_c, where N is the number of nearest neighbors and V_c is the volume of a cell. We approximate the average of NV_c by the product of the average number of neighbor cells [15·54 for the Voronoi construction (Meijering, 1953)] and the average cell volume ($1/c$). In terms of the characteristic length,

$$\int_0^\infty 4\pi r^2 p_1(r)\mathrm{d}r = 15{\cdot}54c^{-1} = 15{\cdot}54(4l/\pi)^3. \tag{33}$$

We assume the algebraic form

$$p_1(r) = Kr\exp(-pr), \tag{34}$$

which satisfies conditions (*a*) (*b*) and (*c*), and use the remaining conditions to fix the parameters K and p. The initial slope condition (*d*) means that

$$K = \tfrac{8}{9}(9\pi c/16)^{1/3}\Gamma(\tfrac{2}{3}) = 1{\cdot}45522c^{1/3}. \tag{35}$$

From condition (*e*)

$$K\int_0^\infty r^3\exp(-pr)\mathrm{d}r = K(4!)/4p^4 = 15{\cdot}54/(4\pi c). \tag{36}$$

Then $p = 1{\cdot}6301c^{1/3}$.

When $\gamma(r)$ is constructed using (32) and (34), the scattering intensity, from Fourier transforming and slit smearing, becomes

$$\tilde{I}_t(h) = 4\pi l^2 F(hl) + 57{\cdot}450c^{1/3}(1 - \psi_{21}/\varphi_2) \times (5{\cdot}3144c^{2/3} - h^2)(2{\cdot}6572c^{2/3} + h^2)^{-5/2} \tag{37}$$

for a two-phase system. The first term is the intensity corresponding to $p_0(r)$ for a Voronoi cell density c and characteristic length $l = (\pi c/4)^{-1/3}$. This may be rewritten as

$$\tilde{I}_t(h) = l^2[4\pi F(hl) + 62{\cdot}267(1 - \psi_{21}/\varphi_2) \times (6{\cdot}2430 - h^2l^2)(2{\cdot}8800 + h^2l^2)^{-5/2}]. \tag{38}$$

With an overall multiplying constant C, this is a three-parameter model, the other parameters being the length l and the correlation factor ψ_{21}.

On minimizing Q with respect to these parameters for SiO_2 we find $l = 88{\cdot}38$ Å and $1 - \psi_{21}/\varphi_2 = 0{\cdot}0551$. The value of Q is 2956, to be compared with a value of 5666 obtained with no intercell correlation. The initial slope of γ is

$$\gamma'(0) = (-1{\cdot}57724/l) + (1 - \psi_{21}/\varphi_2)(1{\cdot}57724/l) = -0{\cdot}01685\ \text{Å}^{-1}.$$

With respect to the correlation, we note that ψ_{21} is almost 95% of φ_2, so there is a small tendency for neighbors of cells filled with SiO_2 to also contain SiO_2, which is physically reasonable. The length l is about 6% smaller than for the uncorrelated model: smaller cells plus positive intracell correlations tend to keep the average size of the pieces of silica the same in both models. Considering Al_2O_3, we find $Q = 3169$ (one Voronoi, with two parameters, gave $Q = 8791$ with $l = 93{\cdot}65$ Å). The characteristic length is found to be 83·54 Å and the correlation parameter $1 - \psi_{21}/\varphi_2$ is 0·0565, so that there seems to

be about the same correlation between cells (enhanced probability of neighboring cells having the same contents) as is the case for SiO_2. The single-Voronoi model gives $\gamma'(0) = -0{\cdot}01760\ \text{Å}^{-1}$; the correlated Voronoi gives $\gamma'(0) = -0{\cdot}01695\ \text{Å}^{-1}$. As also reflected in S^2 (Table 2), the correlation factor is an improvement in the model, and thus gives a better description of the arrangement of electron density, even when the addition of adjustable parameters is taken into account.

III. Three-phase system

We now turn to the three-phase catalyst, containing platinum as well as support and void. We will first consider curve fitting to the scattering intensities, with no model, then cell-based models, and finally models which relate the structure of the catalyst to the structure of the support.

At the outset, we note that it is impossible to determine the individual P_{ij} from the X-ray scattering alone, since (6) constitutes one equation for three unknown functions. Even if one writes

$$\gamma = Q_{12}f_{12}(r) + Q_{13}f_{13}(r) + Q_{23}f_{23}(r) \qquad (39)$$

and parametrizes the three functions f_{ij} to get a good fit between the Fourier transform of γ and the experimental scattering, one cannot identify f_{ij} with γ_{ij}: there are an infinite number of sets of f_{ij} which give exactly the same γ for a given set of Q_{ij}. The interphase surface areas per unit volume are given by

$$S_{ij}/4V = (\mathrm{d}P_{ij}/\mathrm{d}r)_{r=0} = -\varphi_i\varphi_j\gamma'_{ij}(0). \qquad (40)$$

Thus, rigorously, we cannot determine the three surface areas without additional information or the use of a model. A physical model will yield the individual P_{ij}, and hence values for the three individual surfaces.

If we write $\gamma(r)$ as (6), for Pt/SiO_2, the coefficients are: $Q_{12} = 0{\cdot}8720$, $Q_{13} = 0{\cdot}0179$, $Q_{23} = 0{\cdot}1101$. From (6) and (7), for Pt/SiO_2,

$$\gamma'(0) = -\sum_{i<j} Q_{ij}P'_{ij}(0)/\varphi_i\varphi_j$$

$$= -(6{\cdot}031S_{12} + 283S_{13} + 371S_{23})/4V. \qquad (41)$$

From the experimental data, we evaluate $\tilde{k}$ as $3{\cdot}827\ \text{Å}^{-3}$ and $\tilde{Q} = \int h\tilde{I}(h)\mathrm{d}h$ as $183{\cdot}6\ \text{Å}^{-2}$. Thus $\gamma'(0) = -0{\cdot}02084\ \text{Å}^{-1}$. If we approximate S_{12}/V by $0{\cdot}01149\ \text{Å}^{-1}$, from the SiO_2 scattering, the term $-6{\cdot}031S_{12}/4V$ would be $-0{\cdot}0173\ \text{Å}^{-1}$, *i.e.* 5/6 $\gamma'(0)$. The Pt/Al_2O_3 catalyst scattering gives $\tilde{k}/\tilde{Q} = 0{\cdot}0224(17)\ \text{Å}^{-1} = -\gamma'(0)$ so that ($Q_{12} = 0{\cdot}8543$, $Q_{13} = 0{\cdot}01701$, $Q_{23} = 0{\cdot}1287$)

$$0{\cdot}0896\ \text{Å}^{-1} = \sum_{ij} Q_{ij}S_{ij}/V\varphi_i\varphi_j$$

$$= 5{\cdot}923S_{12}/V + 82{\cdot}33S_{13}/V + 132{\cdot}4S_{23}/V. \qquad (42)$$

With the value $0{\cdot}01086\ \text{Å}^{-1}$ for S_{12}/V, from the alumina scattering, the term $5{\cdot}923S_{12}/V$ is $0{\cdot}0644\ \text{Å}^{-1}$, about 3/4 of the left side of (42). For both silica and alumina supports, the support–void surfaces are the largest contributors to $\gamma'(0)$, but are far from dominating it totally. The large weights on S_{13}/V and S_{23}/V (owing to the high electron density contrast) mean that these surfaces are several orders of magnitude smaller than S_{12}/V.

(*a*) *Fitting functions*

Fitting experimental intensities for Pt/SiO_2 to various functions serves to ascertain how many parameters can be determined. With a single exponential, a functional form that proved not particularly appropriate for the silica system, $Q = 2{\cdot}08 \times 10^4$ with $l = 37{\cdot}12$ Å. An attempt to use several exponentials led to all exponential parameters becoming identical and little improvement in Q. A fit to a single Voronoi noncrossing function (the calculated intensity again involves two variable parameters) gave a much better Q, 8791, and a length 94·76 Å, so $\gamma'(0) = -0{\cdot}0166\ \text{Å}^{-1}$. A sum of two Voronoi functions gives $Q = 430$, lengths 133·9 and 75·4 Å, and $\gamma'(0) = -0{\cdot}0181\ \text{Å}^{-1}$. With three Voronoi functions (six parameters) we have a fit to experimental error by the criterion that the deviations between fitted and experimental intensities, relative to $\tilde{I}^{1/2}$, are almost statistical: almost half the values are within unity. We find $Q = 133$; the lengths are 130·5, 75·8 and 12·1 Å, and $\gamma'(0) = -0{\cdot}02264\ \text{Å}^{-1}$. Parameters of $\gamma(r)$ obtained from functions with six or more variable parameters can, thus, not be taken seriously.

Fitting the Pt/Al_2O_3 scattering to a single Voronoi function gives $l = 84{\cdot}0$ Å, $Q = 19966$. Two Voronois give $Q = 1882$ ($l = 67{\cdot}0$, 130·4 Å) and three Voronois $Q = 412$ ($l = 52{\cdot}51$, 87·87, 193·76 Å). The values of $\gamma'(0)$ for the three functions are, respectively: $-0{\cdot}01878$, $-0{\cdot}02039$, $-0{\cdot}02092\ \text{Å}^{-1}$. Surprisingly, a sum of an exponential and a Gaussian (four parameters in $\tilde{I}_t$) gives $Q = 237$, and $\gamma'(0) = -0{\cdot}02047\ \text{Å}^{-1}$. In spite of the low Q values, the discrepancies between $\gamma'(0)$ values and $\tilde{k}/\tilde{Q}$ imply a problem with the Pt/Al_2O_3 scattering intensities at high h. In fact, the intensities for high h do not fall off as fast as those for the other samples.

One may also obtain a fit to $\gamma(r)$ by using calculated Q_{ij}, and parametrizing the f_{ij} in (39). Equation (6) suggests that the function used for each f_{ij} must be unity at $r = 0$ and approach 0 for $r \to \infty$; it *probably* should be monotonic and positive everywhere. If each f_{ij} is taken as an exponential, one finds all three exponential parameters approximately identical and the fit is poor. If each is taken as a Voronoi noncrossing function, one has a four-parameter fit to $\tilde{I}$, which for Pt/SiO_2 gives $Q = 1122$, $\gamma'(0) = -0{\cdot}01774\ \text{Å}^{-1}$. If each is a function of the form (21),

Table 3. *Surface areas for three-phase systems in* $Å^{-1}$

Model	Results for Pt/SiO_2			Results for Pt/Al_2O_3		
	S_{12}/V	S_{13}/V	S_{23}/V	S_{12}/V	S_{13}/V	S_{23}/V
Debye-random	0·0155	$6·8 \times 10^{-6}$	$3·2 \times 10^{-5}$	0·0163	$2·33 \times 10^{-5}$	$1·10 \times 10^{-4}$
Simple Voronoi	0·00963	$4·2 \times 10^{-6}$	$1·98 \times 10^{-5}$	0·01083	$1·55 \times 10^{-5}$	$7·30 \times 10^{-5}$
Two-size Voronoi*	0·00929	$4·1 \times 10^{-6}$	$4·22 \times 10^{-5}$	0·01012	$1·45 \times 10^{-5}$	$1·698 \times 10^{-4}$
Two-size Voronoi†	0·01020	$4·4 \times 10^{-6}$	$2·57 \times 10^{-5}$	0·01142	$1·64 \times 10^{-5}$	$9·79 \times 10^{-5}$
Correlated Voronoi‡	0·00955	$2·3 \times 10^{-6}$	$1·06 \times 10^{-5}$	0·01042	$1·49 \times 10^{-5}$	$7·01 \times 10^{-5}$
Correlated Voronoi§	0·01000	$2·3 \times 10^{-6}$	$1·06 \times 10^{-5}$	0·00977	$0·65 \times 10^{-5}$	$3·04 \times 10^{-5}$

*Support in large cells, metal and void in small cells.
†Support in both large and small cells.
‡Assuming ψ_{ij}/φ_i is the same for all i and j.
§Approximating S_{13} and S_{23} in calculation of S_{12}, and approximating S_{12} in calculation of S_{13} and S_{23}.

we have $Q = 665$, but there are now seven parameters in $\tilde{I}$, so one must conclude (remembering the three-Voronoi result) that the functions (21) are not particularly good for the system. The slope $\gamma'(0)$ is $-0·0181$ $Å^{-1}$.

Similarly, for Pt/Al_2O_3, writing γ as a sum of three Voronoi functions weighted by Q_{ij} (6) gives $Q = 2703$ and $\gamma'(0) = -0·01998$ $Å^{-1}$ (four parameters in $\tilde{I}_t$); use of the sine-exponential gives $Q = 483$ and $\gamma'(0) = -0·02113$ $Å^{-1}$ (this is a seven-parameter function). However, without a model showing why each f_{ij} should be identified with the corresponding γ_{ij}, we are unwilling to report surface areas calculated from functions like (39).

(*b*) *Models*

The simplest model is the 'Debye-random' (Goodisman & Brumberger, 1971; Ciccariello, 1983), which predicts (*a*) a single exponential represents $\gamma(r)$ and (*b*) each surface S_{ij} is proportional to the corresponding product $\varphi_i\varphi_j$. Recognizing that prediction (*a*) is not well borne out, we anticipate that the surface areas calculated according to this model are unreliable. Nevertheless, we give the results, according to

$$S_{ij} = 4VP'_{ij}(0) = -4V\gamma'_{ij}(0)\varphi_i\varphi_j, \tag{43}$$

where $\gamma'_{ij}(0) = -1/37·13$ $Å^{-1}$ for all i and j for Pt/SiO_2, so that $S_{12}/V = 0·0155$, $S_{13}/V = 6·8 \times 10^{-6}$, $S_{23}/V = 3·2 \times 10^{-5}$ $Å^{-1}$. The first value resembles what the 'Debye-random' or exponential model gave for the two-phase support, $4(0·0270)\varphi_1\varphi_2 = 0·0156$ $Å^{-1}$. Corresponding results for Pt/Al_2O_3 are given in Table 3. Since $\gamma'(0) = -0·02796$ $Å^{-1}$, S_{12}/V is 0·0163 $Å^{-1}$, which is close to the value given by this model for unmetallized support, 0·0170 $Å^{-1}$.

We now turn to models based on Voronoi cells. The simplest, with a single cell size and random filling, predicts $\gamma(r) = p_0(r)$, the noncrossing function for Voronoi cells, and $\gamma_{ij} = p_0(r)$ for all i and j. Thus, $S_{ij} = 6·309V\varphi_i\varphi_j/l$ according to (25) and (43). For Pt/SiO_2, $l = 94·76$ Å, so that $S_{12}/V = 0·00963$, $S_{13}/V = 4·21 \times 10^{-6}$, $S_{23}/V = 1·98 \times 10^{-5}$ $Å^{-1}$. The Q value is 8791. For Pt/Al_2O_3 we find $l = 84·0$ Å; see Table 3 for calculated surfaces. The simple Voronoi cell model gave $S_{12}/V = 0·00967$ for SiO_2 and 0·00974 $Å^{-1}$ for Al_2O_3. For Pt/Al_2O_3, S_{12} is significantly larger than for unmetallized support. This and the high Q (9966) suggest that the model does not apply well to this sytem.

Since the metal is deposited on an already-formed support, it is reasonable to use two cell sizes, the first characterizing the support and the second characterizing the metal. The smaller cells represent a division of the larger, edge effects and lack of fit being ignored. By considering the various contributions to each P_{ij}, we find

$$P_{12}/\varphi_1\varphi_2 = P_{13}/\varphi_1\varphi_3 = 1 - p_0^{(b)}, \tag{44a}$$

where $p_0^{(b)}$ is the noncrossing function for big cells, and

$$P_{23}/\varphi_2\varphi_3 = 1 - p_0^{(b)} + (p_0^{(b)} - p_0^{(s)})/(\varphi_2 + \varphi_3), \tag{44b}$$

where $p_0^{(s)}$ is the noncrossing function for small cells. This means that γ_{12} and γ_{13} are each just $p_0^{(b)}$, while γ_{23} is $p_0^{(b)} + (\varphi_2 + \varphi_3)^{-1}(p_0^{(s)} - p_0^{(b)})$. Combining these, we construct the correlation function which, for Pt/SiO_2, becomes

$$\gamma(r) = 0·8665p_0^{(b)} + 0·1335p_0^{(s)}.$$

With the three-parameter intensity function corresponding to this $\gamma(r)$, we obtain $Q = 3063$. The large and small cells have characteristic lengths of 98·22 and 49·08 Å, so the initial slope $\gamma'(0)$ is

$$-1·57724\left(\frac{0·8665}{98·22} + \frac{0·1335}{49·8}\right) = -0·01814 \text{ Å}^{-1}$$

and the individual surface areas [see (44)] are as follows: $S_{12}/V = 4\varphi_1\varphi_2(1·5772)/98·22 = 0·00929$, $S_{13}/V = 4·1 \times 10^{-6}$ $Å^{-1}$, $S_{23}/V = 4(1·5772)(51·74^{-1} - 0·1754/100·6)\varphi_2\varphi_3/(\varphi_2 + \varphi_3)$. The first two surfaces are not much changed from the single-cell model; Q is hardly improved either. For Pt/Al_2O_3 (see Table 3), the situation is similar. The large value of Q (9565) suggests the surfaces are not very reliable.

This model can be improved by allowing some of the support to be in small cells, corresponding to the

two-cell-size model which was successful for the support. This is achieved by considering a four-phase two-cell-size system with the first phase in large cells and the remaining phases in small cells, subsequently putting the electron densities of the first and fourth phases equal, as discussed elsewhere (Brumberger & Goodisman, 1983). A new parameter f enters the correlation function, representing the fraction of support found in small cells. The stick probability functions are as follows for this model:

$$P_{1j}/\varphi_1\varphi_j = 1 - p_0^{(b)} + f(p_0^{(b)} - p_0^{(s)})/(1 - \varphi_1 + f\varphi_1) \tag{45}$$

($j = 2, 3$) and

$$P_{23}/\varphi_2\varphi_3 = 1 - p_0^{(b)} + (p_0^{(b)} - p_0^{(s)})/(1 - \varphi_1 + f\varphi_1). \tag{46}$$

Calculating $\gamma(r)$ and $\tilde{I}_t$, and minimizing Q with respect to the four parameters (l_b, l_s, f, and the multiplier C), we get $Q = 430$ for Pt/SiO_2. Furthermore, almost half the deviations of $\tilde{I}_t$ from $\tilde{I}$ are within $\tilde{I}^{1/2}$; we consider this model probably describes the system well. The value of f is 0·595 (about 2/5 of the support in large cells), and the lengths are: $l_b = 133{\cdot}9$, $l_s = 75{\cdot}4$ Å, differing by a factor of about two. The surface areas are

$$S_{12}/V = 4\varphi_1\varphi_2(1{\cdot}5772)\left[\frac{1}{l_b} - \frac{f}{1 - \varphi_1 + f\varphi_1}\left(\frac{1}{l_b} - \frac{1}{l_s}\right)\right]$$

$$S_{13} = \varphi_3 S_{12}/\varphi_2$$

$$S_{23}/V = 4\varphi_2\varphi_3(1{\cdot}5772)\left[\frac{1}{l_b} - \frac{l_b^{-1} - l_s^{-1}}{1 - \varphi_1 + f\varphi_1}\right].$$

For the Pt/SiO_2 system, we find $S_{12}/V = 0{\cdot}01020$, $S_{13}/V = 4{\cdot}45 \times 10^{-6}$, $S_{23}/V = 2{\cdot}57 \times 10^{-5}$ Å^{-1}. For Pt/Al_2O_3, we find $Q = 1882$, $l_b = 130{\cdot}4$, $l_s = 66{\cdot}98$ Å, $f = 0{\cdot}629$, and the surface areas given in Table 3.

A final cell model is the correlated cell model. For Pt/SiO_2, according to (32), the correlation function is

$$\gamma(r) = p_0(r) + p_1(r)(1 - 1{\cdot}0580\psi_{21} - 49{\cdot}590\psi_{31} - 306{\cdot}00\psi_{32}). \tag{47}$$

The quantity in parentheses in (47) is a single parameter, which we denote by D. D = zero for no correlation ($\psi_{21} = \varphi_2$, $\psi_{31} = \varphi_3$, $\psi_{32} = \varphi_3$). Thus three parameters are to be varied in minimizing the deviation between experimental and theoretical scattering intensities, just as for the two-phase system. The best value of Q, 3283, is slightly higher than for the two-phase system. It is obtained with a cell length of 84·73 Å and $D = 0{\cdot}1126$. There is thus a slight positive correlation between cells (enhanced probability for neighbor cells to have the same contents). For Pt/Al_2O_3, introduction of a correlation factor reduces Q from 9966 (single Voronoi) to 6899 with $l = 73{\cdot}3$ Å and the coefficient D equal to 0·1609. This gives $\gamma'(0) = -0{\cdot}0181$ Å^{-1}, and a somewhat larger positive correlation between contents of neighboring cells.

The interphase surface areas are given by

$$S_{ij}/V = \tfrac{1}{2}(\psi_{ij}\varphi_j + \psi_{ji}\varphi_i)(6{\cdot}309/l). \tag{48}$$

To derive individual ψ_{ij}'s from the parameter D requires an additional assumption. For instance, one can assume that ψ_{ij}/φ_i is the same for all i and j. Then with $D = 0{\cdot}1126$

$$0{\cdot}8874 = 1{\cdot}058\psi_{21} + 49{\cdot}590\varphi_3\psi_{21}/\varphi_2 + 306{\cdot}00\varphi_3\psi_{21}/\varphi_2$$

or $\psi_{21} = 0{\cdot}7314$. We can now calculate surface areas according to (48), obtaining $S_{12}/V = 0{\cdot}00955$, $S_{13}/V = 4{\cdot}17 \times 10^{-6}$, $S_{32}/V = 1{\cdot}96 \times 10^{-5}$ Å^{-1}. For Pt/Al_2O_3, the assumption of constant ψ_{ij}/φ_i leads to the equation

$$0{\cdot}8391 = 1{\cdot}0371\psi_{21} + 14{\cdot}412\varphi_3\psi_{21}/\varphi_2 + 109{\cdot}06\varphi_3\psi_{21}/\varphi_2$$

so that $\psi_{21} = 0{\cdot}6912$. Then the surface areas, using (48) with $l = 72{\cdot}7$ Å, are $S_{12}/V = 0{\cdot}01042$, $S_{13}/V = 1{\cdot}49 \times 10^{-5}$, $S_{23}/V = 7{\cdot}01 \times 10^{-5}$ Å^{-1}.

Another way to get individual surface areas from the correlated-cell model is to approximate one in calculating others. Writing D in terms of surface areas, using (48), we have for Pt/SiO_2

$$0{\cdot}0661 \text{ Å}^{-1} = (6{\cdot}030S_{12} + 282{\cdot}7S_{13} + 371{\cdot}3S_{23})/V. \tag{49}$$

We expect S_{13} and S_{23} to be several orders of magnitude smaller than S_{12}; their contribution to the above equation is less than 0·01. Using S_{13}/V and S_{23}/V values obtained for two-size Voronoi with support in large and small cells, we calculate S_{12}/V for Pt/SiO_2 as 0·01000 Å^{-1}. For Pt/Al_2O_3 we have

$$0{\cdot}0709 \text{ Å}^{-1} = (5{\cdot}923S_{12} + 82{\cdot}31S_{13} + 132{\cdot}40S_{23})/V \tag{50}$$

and approximating S_{13} and S_{23} gives $S_{12} = 0{\cdot}00977$ Å^{-1}. To calculate S_{13} and S_{23}, one could approximate S_{12} in (49) or (50) by its value for the two-size Voronoi. Then one could assume $S_{13}/S_{23} = \varphi_1/\varphi_2$ to obtain values for the individual surfaces. Results of this procedure are in Table 3. A problem is that a small uncertainty in the value of S_{12} used becomes a large error in S_{13} and S_{23}, and the values are only half what other models give.

Reviewing the areas of Table 3, we note that (except for the Debye-random model, already dismissed as a poor one for this system) the models discussed are fairly consistent in the values for the support–void and support–metal surfaces. Values for the metal–void surface vary most, over a factor of two. The two-size Voronoi with support in large and small cells is the

Table 4. *Specific surfaces in* $m^2\ g^{-1}$

System	S^*_{12}	S^*_{13}	S^*_{23}
SiO_2†	299	–	–
Pt/SiO_2‡	251(8)	0·109(3)	0·69(24)
Al_2O_2†	166	–	–
Pt/Al_2O_3‡	158(9)	0·230(11)	1·55(61)

†From $\tilde{k}/\tilde{Q}$.
‡Average of all results of Table 3 except Debye-random, with error the mean-square deviation from the average.

best model, judged by the small Q and the fact that it requires no extra assumptions to derive surface areas. It gives metal–void surface areas in the middle of the range of values of the models. The method in the next section turns out to be best for the metal–void surface. Dropping the Debye-random results and the S_{13} and S_{23} results for the last model discussed, we have averaged the results of the different models, calculated the mean-square deviation from the mean and converted to specific surfaces in $m^2\ g^{-1}$ by multiplying by 10^4 and dividing by mass density. This yields Table 4.

(c) *Support subtraction*

A different sort of model (Goodisman, Brumberger & Cupelo, 1981; Brumberger, Delaglio, Goodisman, Phillips, Schwarz & Sen, 1985) involves the use of measurements on metallized support as well as on the catalyst. It is assumed that the addition of metal to the support, which gives the catalyst, does not change the support structure, so that, for example, the sum of the support–void and the support–metal surface areas in the catalyst is identical to the support–void surface area in the unmetallized support:

$$S^{(3)}_{12} + S^{(3)}_{13} = S^{(2)}_{12}. \tag{51}$$

We here use superscripts to give the number of phases in the system referred to. Evidence for the validity of assumption (51) must come from (*a*) comparison of the densities of support and catalyst and (*b*) consideration of the analyzed scattering of the two systems. Since there are three surfaces in the catalyst and one in the support, use of (51) still does not suffice for the determination of the individual surfaces; some additional assumption is necessary. However, the value of the metal–void surface $S^{(3)}_{23}$ turns out to be insensitive to the assumption made.

It is convenient to introduce the parameter r, the ratio between the exposed and covered metal surfaces, or $S^{(3)}_{23}/S^{(3)}_{13}$. It then can be shown (Brumberger *et al.*, 1985) that

$$[\overline{\eta^2}\gamma'(0)]^{(2)} - [\overline{\eta^2}\gamma'(0)]^{(3)} = [-S^{(3)}_{13}/4V](2n_1n_3 - n_3^2 - rn_3^2) \tag{52}$$

and $S^{(3)}_{23}$ is just $rS^{(3)}_{13}$. The value of r would be unity if the metal were in extended layers with lateral area negligible compared to top and bottom surfaces, and infinite if it were in spheres touching the support at a point only. For hemispherical caps, $r = 2$; for tetrahedra $r = 3$; for cubes $r = 5$.

According to the data of Table 1, $\overline{\eta^2}$ is 0·1729 for the SiO_2 system and 0·1981 for the three-phase catalyst. Then (52) becomes

$$[S^{(3)}_{13}/V](-54{\cdot}80 + 73{\cdot}55r) = 0{\cdot}00277\ \text{Å}^{-1} \tag{53a}$$

and

$$S^{(3)}_{23}/V = (26552 - 19783r^{-1})^{-1}. \tag{53b}$$

Thus, $S^{(3)}_{23}/V$ varies from $14{\cdot}7 \times 10^{-5}$ Å^{-1}, for $r = 1$, to $6{\cdot}00 \times 10^{-5}$ Å^{-1}, for $r = 2$, to $3{\cdot}77 \times 10^{-5}$ Å^{-1} as $r \to \infty$. The insensitivity of this quantity to r for $r > 3$ has been noted previously. This model suggests the value $4{\cdot}3(5) \times 10^{-5}$ Å^{-1}, *i.e.* 1·11(13) m^2 (g of catalyst)$^{-1}$. The surface $S^{(3)}_{13}$ is more sensitive to the value of r, $S^{(3)}_{13}/V$ being $14{\cdot}7 \times 10^{-5}$ Å^{-1} for $r = 1$ and approaching 0 as $r \to \infty$. $S^{(3)}_{12}/V$ is then, using $S^{(2)}_{12}/V = 0{\cdot}01149$ Å^{-1}, between 0·01134 ($r = 1$) and 0·01149 Å^{-1} ($r \to \infty$), *i.e.* the metal can take only a negligible fraction of the support surface. The surface-to-volume ratio for support, $S^{(2)}_{21}/V$, was calculated as 0·01149 Å^{-1} from $\tilde{k}/\tilde{Q}$.

The support-subtraction model applied to Al_2O_3 and Pt/Al_2O_3 leads to the following results:

$$\frac{S^{(3)}_{13}}{V} = \frac{0{\cdot}01408\ \text{Å}^{-1}}{-42{\cdot}43 + 73{\cdot}55r};\ \frac{S^{(3)}_{23}}{V} = \frac{0{\cdot}01408\ \text{Å}^{-1}}{-42{\cdot}43r^{-1} + 73{\cdot}55}. \tag{54}$$

For $r = 3$, $S^{(3)}_{13}/V = 7{\cdot}86 \times 10^{-5}$ Å^{-1} [covered surface of 1·18 m^2 (g of catalyst)$^{-1}$] and $S^{(3)}_{23}/V$ varies from $2{\cdot}36 \times 10^{-4}$ Å^{-1} (free metal surface of 3·55 m^2 (g of catalyst)$^{-1}$] for $r = 3$ to $1{\cdot}90 \times 10^{-4}$ Å^{-1} for $r \to \infty$. For both Pt/SiO_2 and Pt/Al_2O_3, the probable values of $S^{(3)}_{23}/V$ by support subtraction are about twice as large as those from the other models (Table 4). No value of r can give agreement with those models. This suggests support subtraction is not valid, *i.e.* the support in the catalyst differs from unmetallized support, perhaps due to the effect of treatment involved in preparing the catalyst, as was found for TiO_2 (Brumberger *et al.*, 1985).

IV. Conclusions

We have considered fits of theoretical functions $I_t(h)$ to experimental scattering intensities $\tilde{I}(h)$. Accuracy of fit was judged by how small Q (9) could be made, and by the figure of merit F (11), which takes into account the number of adjustable parameters. We found F to be a good guide to applicability of functions. We calculated surface areas from various fitting functions and associated models. These are given as specific surfaces in m^2 (g of catalyst)$^{-1}$, in Table 4.

For the two-phase systems considered, the best simple function for fitting the small-angle X-ray scat-

tering is the exponential-Gaussian, which involves four parameters. A fit to experimental error can be obtained with three Voronois (six parameters). However, if only the surface area is of interest, fitting the scattering is an unnecessary exercise since for a two-phase system the surface area can be obtained directly from the data. Fitting a theoretical result to the scattering is useful if the fitting function derives from a model, since the values determined for its parameters now give information about the structure of the system, the fit of theoretical scattering intensities to experiment becoming an indication of the applicability of the model.

In this context, the Voronoi cell models appear useful in providing a physical picture for the distribution of matter and pores in the SiO_2 or Al_2O_3 samples considered. Introduction of a correlation factor, or use of a two-cell-size model, seems to provide a reasonable description for SiO_2 and Al_2O_3. We must note that there is a limit on the information obtainable from a model since, with six parameters, a fitting function can give scattering intensities in agreement with experiment to experimental error. One would not want to take seriously values of parameters for a model with more than six parameters.

For a system with more than two phases, there is no way of obtaining individual surface areas from the scattering intensities *without* a model. If the correlation function is written in the form of (6)–(8), we require the individual γ_{ij} to obtain surface areas, as seen in (5). However, parametrizing functions in a form like (39) is not useful unless one has a theoretical basis, *i.e.* a model, for assuming that γ_{ij} is of the form assumed for f_{ij}. Given a model for the γ_{ij}, comparison of the value of Q with what one can obtain with other forms for γ gives an idea of whether the model is a good description of the system, so that its parameters can be taken seriously, or whether one is just curve fitting.

We have considered cell models of varying degrees of complexity, after rejecting the Debye-random model because of the poor Q value. The best model is that involving two Voronoi cell sizes with support in both large and small cells. Its problem is the assumption that edge effects may be ignored when l_b/l_s is not large. On the other hand, small l_b/l_s means it is unlikely that there will be isolated metal-filled cells surrounded by void, which would be unphysical. The correlated cell model is free from the edge-effect problem, but requires additional assumptions to yield surface areas. We have shown how different assumptions affect the results: the surface S_{12} hardly changes, but the metal surfaces may vary by 50%. The surface areas obtained from five models have been averaged to give the specific surfaces in Table 4, and an uncertainty has been calculated as the mean-square deviation from the mean. It is seen that the other surfaces are reliable (independent of model) to about 5% for Pt/SiO_2 and 20% for Pt/Al_2O_3. It may be noted that the ratio $r = S^*_{23}/S^*_{13}$ is about six for both catalysts. A value of 6 for r corresponds to cube-like metal particles sitting on a face ($r = 5$ for cubes). Inconsistencies between support-subtraction results and other results suggest the support was changed during catalyst preparation. However, note that S^*_{12} in each case is about equal to its value for the corresponding unmetallized support (errors in $\tilde{k}/\tilde{Q}$ were estimated as 13 and 11 $m^2\ g^{-1}$ in §II), so experimental errors may have a large effect.

The samples were kindly sent to us by Professor J. B. Cohen and Dr R. K. Nandi of the Materials Science Group at Northwestern University, where the samples were characterized by various techniques and the SAXS measured. This work was supported by the National Science Foundation under grant no. CPE-7913779.

References

BRUMBERGER, H. (1983). *Trans. Am. Crystallogr. Assoc.* **19**, 1–16.

BRUMBERGER, H., DELAGLIO, F., GOODISMAN, J., PHILLIPS, M. G., SCHWARZ, J. A. & SEN, P. (1985). *J. Catal.* **92**, 199–210.

BRUMBERGER, H. & GOODISMAN, J. (1983). *J. Appl. Cryst.* **16**, 83–88.

CICCARIELLO, S. (1983). *Phys. Rev. B*, **28**, 4301–4306.

CICCARIELLO, S. (1984). *J. Appl. Phys.* **56**, 162–167.

CICCARIELLO, S. & BENEDETTI, A. (1985). *J. Appl. Cryst.* **18**, 219–229.

CICCARIELLO, S., COCCO, G., BENEDETTI, A. & ENZO, S. (1981). *Phys. Rev. B*, **23**, 6474–6485.

COPPA, N. & GOODISMAN, J. (1981). *J. Appl. Cryst.* **14**, 309–314.

DANIEL, C. & WOOD, F. S. (1971). *Fitting Equations to Data.* New York: Wiley-Interscience.

DEBYE, P., ANDERSON, H. R. JR & BRUMBERGER, H. (1957). *J. Appl. Phys.* **28**, 679–683.

DELAGLIO, F., GOODISMAN, J. & BRUMBERGER, H. (1986). *J. Catal.* In the press.

GOODISMAN, J. & BRUMBERGER, H. (1971). *J. Appl. Cryst.* **4**, 347–351.

GOODISMAN, J. & BRUMBERGER, H. (1979). *J. Appl. Cryst.* **12**, 398–399.

GOODISMAN, J., BRUMBERGER, H. & CUPELO, R. (1981). *J. Appl. Cryst.* **14**, 305–308.

GOODISMAN, J. & COPPA, N. (1981). *Acta Cryst.* A**37**, 170–180.

KALER, E. W. & PRAGER, S. (1982). *J. Colloid Interface Sci.* **86**, 359–369.

MEIJERING, J. L. (1953). *Philips Res. Rep.* **8**, 270–290.

NANDI, R. K. (1984). Private communication.

NANDI, R. K., MOLINARO, F., TANG, C., COHEN, J. B., BUTT, J. B. & BURWELL, R. L. (1982). *J. Catal.* **78**, 289–305.

PETERLIN, A. (1965). *Makromol. Chem.* **87**, 152–165.

POROD, G. (1951). *Kolloid Z.* **124**, 83–114.

POROD, G. (1982). *Small-Angle X-ray Scattering*, edited by O. GLATTER & O. KRATKY. New York: Academic Press.

RULAND, W. (1971). *J. Appl. Cryst.* **4**, 70–73.